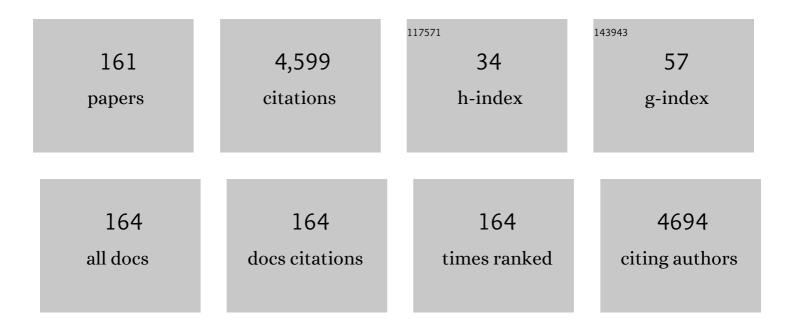
List of Publications by Year in descending order

Source: https://exaly.com/author-pdf/1587683/publications.pdf Version: 2024-02-01



IOHN I TANNER

#	Article	IF	CITATIONS
1	Artificial intelligence in the prediction of protein–ligand interactions: recent advances and future directions. Briefings in Bioinformatics, 2022, 23, .	3.2	78
2	Structure-affinity relationships of reversible proline analog inhibitors targeting proline dehydrogenase. Organic and Biomolecular Chemistry, 2022, 20, 895-905.	1.5	6
3	Impact of missense mutations in the ALDH7A1 gene on enzyme structure and catalytic function. Biochimie, 2021, 183, 49-54.	1.3	1
4	Structural analysis of prolines and hydroxyprolines binding to the l-glutamate-γ-semialdehyde dehydrogenase active site of bifunctional proline utilization A. Archives of Biochemistry and Biophysics, 2021, 698, 108727.	1.4	6
5	Biochemical Characterization of the Two-Component Flavin-Dependent Monooxygenase Involved in Valanimycin Biosynthesis. Biochemistry, 2021, 60, 31-40.	1.2	6
6	Structure, biochemistry, and gene expression patterns of the proline biosynthetic enzyme pyrroline-5-carboxylate reductase (PYCR), an emerging cancer therapy target. Amino Acids, 2021, 53, 1817-1834.	1.2	20
7	Disease variants of human Δ1-pyrroline-5-carboxylate reductase 2 (PYCR2). Archives of Biochemistry and Biophysics, 2021, 703, 108852.	1.4	9
8	N-Propargylglycine: a unique suicide inhibitor of proline dehydrogenase with anticancer activity and brain-enhancing mitohormesis properties. Amino Acids, 2021, 53, 1927-1939.	1.2	5
9	Structural basis for the stereospecific inhibition of the dual proline/hydroxyproline catabolic enzyme ALDH4A1 by transâ€4â€hydroxyâ€Lâ€proline. Protein Science, 2021, 30, 1714-1722.	3.1	4
10	Structural and Biochemical Characterization of the Flavin-Dependent Siderophore-Interacting Protein from <i>Acinetobacter baumannii</i> . ACS Omega, 2021, 6, 18537-18547.	1.6	5
11	Optimisation of Neuraminidase Expression for Use in Drug Discovery by Using HEK293-6E Cells. Viruses, 2021, 13, 1893.	1.5	1
12	Photoinduced Covalent Irreversible Inactivation of Proline Dehydrogenase by S-Heterocycles. ACS Chemical Biology, 2021, 16, 2268-2279.	1.6	2
13	Probing the function of a ligand-modulated dynamic tunnel in bifunctional proline utilization A (PutA). Archives of Biochemistry and Biophysics, 2021, 712, 109025.	1.4	3
14	Evidence for Proline Catabolic Enzymes in the Metabolism of Thiazolidine Carboxylates. Biochemistry, 2021, 60, 3610-3620.	1.2	0
15	Kinetics of human pyrroline-5-carboxylate reductase in l-thioproline metabolism. Amino Acids, 2021, 53, 1863-1874.	1.2	0
16	Structural and biochemical consequences of pyridoxineâ€dependent epilepsy mutations that target the aldehyde binding site of aldehyde dehydrogenase ALDH 7A1. FEBS Journal, 2020, 287, 173-189.	2.2	7
17	Structural analysis of pathogenic mutations targeting Glu427 of ALDH7A1, the hot spot residue of pyridoxineâ€dependent epilepsy. Journal of Inherited Metabolic Disease, 2020, 43, 635-644.	1.7	6
18	DeepCryoPicker: fully automated deep neural network for single protein particle picking in cryo-EM. BMC Bioinformatics, 2020, 21, 509.	1.2	30

#	Article	IF	CITATIONS
19	Trapping conformational states of a flavin-dependent N-monooxygenase in crystallo reveals protein and flavin dynamics. Journal of Biological Chemistry, 2020, 295, 13239-13249.	1.6	13
20	Inhibition, crystal structures, and in-solution oligomeric structure of aldehyde dehydrogenase 9A1. Archives of Biochemistry and Biophysics, 2020, 691, 108477.	1.4	15
21	In crystallo screening for proline analog inhibitors of the proline cycle enzyme PYCR1. Journal of Biological Chemistry, 2020, 295, 18316-18327.	1.6	22
22	Cautionary Tale of Using Tris(alkyl)phosphine Reducing Agents with NAD ⁺ -Dependent Enzymes. Biochemistry, 2020, 59, 3285-3289.	1.2	7
23	Structural Determinants of Flavin Dynamics in a Class B Monooxygenase. Biochemistry, 2020, 59, 4609-4616.	1.2	8
24	Structure and function of a flavin-dependent S-monooxygenase from garlic (Allium sativum). Journal of Biological Chemistry, 2020, 295, 11042-11055.	1.6	14
25	Covalent Modification of the Flavin in Proline Dehydrogenase by Thiazolidine-2-Carboxylate. ACS Chemical Biology, 2020, 15, 936-944.	1.6	10
26	SAXSDom: Modeling multidomain protein structures using smallâ€angle Xâ€ray scattering data. Proteins: Structure, Function and Bioinformatics, 2020, 88, 775-787.	1.5	9
27	Bioinformatics Methods for Mass Spectrometry-Based Proteomics Data Analysis. International Journal of Molecular Sciences, 2020, 21, 2873.	1.8	134
28	Impaired folate binding of serine hydroxymethyltransferase 8 from soybean underlies resistance to the soybean cyst nematode. Journal of Biological Chemistry, 2020, 295, 3708-3718.	1.6	13
29	A Super-Clustering Approach for Fully Automated Single Particle Picking in Cryo-EM. Genes, 2019, 10, 666.	1.0	12
30	AutoCryoPicker: an unsupervised learning approach for fully automated single particle picking in Cryo-EM images. BMC Bioinformatics, 2019, 20, 326.	1.2	33
31	Structural and Biochemical Characterization of Aldehyde Dehydrogenase 12, the Last Enzyme of Proline Catabolism in Plants. Journal of Molecular Biology, 2019, 431, 576-592.	2.0	20
32	Crystal Structure of Aldehyde Dehydrogenase 16 Reveals Trans-Hierarchical Structural Similarity and a New Dimer. Journal of Molecular Biology, 2019, 431, 524-541.	2.0	15
33	Structural Biology of Proline Catabolic Enzymes. Antioxidants and Redox Signaling, 2019, 30, 650-673.	2.5	37
34	The Proline Cycle As a Potential Cancer Therapy Target. Biochemistry, 2018, 57, 3433-3444.	1.2	107
35	Determination of protein oligomeric structure from smallâ€angle Xâ€ray scattering. Protein Science, 2018, 27, 814-824.	3.1	40
36	Structural Evidence for Rifampicin Monooxygenase Inactivating Rifampicin by Cleaving Its Ansa-Bridge. Biochemistry, 2018, 57, 2065-2068.	1.2	13

#	Article	IF	CITATIONS
37	Flavinâ€N5 Covalent Intermediate in a Nonredox Dehalogenation Reaction Catalyzed by an Atypical Flavoenzyme. ChemBioChem, 2018, 19, 53-57.	1.3	7
38	NAD ⁺ promotes assembly of the active tetramer of aldehyde dehydrogenase 7A1. FEBS Letters, 2018, 592, 3229-3238.	1.3	11
39	Structural Basis for the Substrate Inhibition of Proline Utilization A by Proline. Molecules, 2018, 23, 32.	1.7	9
40	Steric Control of the Rate-Limiting Step of UDP-Galactopyranose Mutase. Biochemistry, 2018, 57, 3713-3721.	1.2	3
41	Redox Modulation of Oligomeric State in Proline Utilization A. Biophysical Journal, 2018, 114, 2833-2843.	0.2	2
42	Impact of disease-Linked mutations targeting the oligomerization interfaces of aldehyde dehydrogenase 7A1. Chemico-Biological Interactions, 2017, 276, 31-39.	1.7	13
43	Structure and characterization of a class 3B proline utilization A: Ligand-induced dimerization and importance of the C-terminal domain for catalysis. Journal of Biological Chemistry, 2017, 292, 9652-9665.	1.6	21
44	Identification of a Conserved Histidine As Being Critical for the Catalytic Mechanism and Functional Switching of the Multifunctional Proline Utilization A Protein. Biochemistry, 2017, 56, 3078-3088.	1.2	5
45	Covalent Allosteric Inactivation of Protein Tyrosine Phosphatase 1B (PTP1B) by an Inhibitor–Electrophile Conjugate. Biochemistry, 2017, 56, 2051-2060.	1.2	22
46	Resolving the cofactor-binding site in the proline biosynthetic enzyme human pyrroline-5-carboxylate reductase 1. Journal of Biological Chemistry, 2017, 292, 7233-7243.	1.6	42
47	Importance of the C-Terminus of Aldehyde Dehydrogenase 7A1 for Oligomerization and Catalytic Activity. Biochemistry, 2017, 56, 5910-5919.	1.2	7
48	Structure, function, and mechanism of proline utilization A (PutA). Archives of Biochemistry and Biophysics, 2017, 632, 142-157.	1.4	56
49	Biophysical investigation of type A PutAs reveals a conserved core oligomeric structure. FEBS Journal, 2017, 284, 3029-3049.	2.2	14
50	Discovery of the Membrane Binding Domain in Trifunctional Proline Utilization A. Biochemistry, 2017, 56, 6292-6303.	1.2	7
51	Multiple functionalities of reduced flavin in the non-redox reaction catalyzed by UDP-galactopyranose mutase. Archives of Biochemistry and Biophysics, 2017, 632, 59-65.	1.4	11
52	Synchrotron-based macromolecular crystallography module for an undergraduate biochemistry laboratory course. Journal of Applied Crystallography, 2016, 49, 2235-2243.	1.9	4
53	The Structure of the Antibiotic Deactivating, N-hydroxylating Rifampicin Monooxygenase. Journal of Biological Chemistry, 2016, 291, 21553-21562.	1.6	36
54	EF5 Is the High-Affinity Mg2+ Site in ALG-2. Biochemistry, 2016, 55, 5128-5141.	1.2	2

#	Article	IF	CITATIONS
55	Structures of Proline Utilization A (PutA) Reveal the Fold and Functions of the Aldehyde Dehydrogenase Superfamily Domain of Unknown Function. Journal of Biological Chemistry, 2016, 291, 24065-24075.	1.6	27
56	Engineering a trifunctional proline utilization A chimaera by fusing a DNA-binding domain to a bifunctional PutA. Bioscience Reports, 2016, 36, .	1,1	6
57	<i>In Crystallo</i> Capture of a Covalent Intermediate in the UDP-Galactopyranose Mutase Reaction. Biochemistry, 2016, 55, 833-836.	1.2	21
58	Empirical power laws for the radii of gyration of protein oligomers. Acta Crystallographica Section D: Structural Biology, 2016, 72, 1119-1129.	1.1	24
59	SAXS fingerprints of aldehyde dehydrogenase oligomers. Data in Brief, 2015, 5, 745-751.	0.5	7
60	X-ray crystal structures of native HIV-1 capsid protein reveal conformational variability. Science, 2015, 349, 99-103.	6.0	212
61	Diethylaminobenzaldehyde Is a Covalent, Irreversible Inactivator of ALDH7A1. ACS Chemical Biology, 2015, 10, 693-697.	1.6	36
62	First Evidence for Substrate Channeling between Proline Catabolic Enzymes. Journal of Biological Chemistry, 2015, 290, 2225-2234.	1.6	37
63	Crystal structure and tartrate inhibition of Legionella pneumophila histidine acid phosphatase. Archives of Biochemistry and Biophysics, 2015, 585, 32-38.	1.4	9
64	Inactivation of protein tyrosine phosphatases by dietary isothiocyanates. Bioorganic and Medicinal Chemistry Letters, 2015, 25, 4549-4552.	1.0	15
65	Contribution to catalysis of ornithine binding residues in ornithine N5-monooxygenase. Archives of Biochemistry and Biophysics, 2015, 585, 25-31.	1.4	13
66	Structural Basis of Substrate Recognition by Aldehyde Dehydrogenase 7A1. Biochemistry, 2015, 54, 5513-5522.	1.2	36
67	Evidence for Hysteretic Substrate Channeling in the Proline Dehydrogenase and Δ1-Pyrroline-5-carboxylate Dehydrogenase Coupled Reaction of Proline Utilization A (PutA). Journal of Biological Chemistry, 2014, 289, 3639-3651.	1.6	28
68	Structures of the PutA peripheral membrane flavoenzyme reveal a dynamic substrate-channeling tunnel and the quinone-binding site. Proceedings of the National Academy of Sciences of the United States of America, 2014, 111, 3389-3394.	3.3	63
69	Contributions of Unique Active Site Residues of Eukaryotic UDP-Galactopyranose Mutases to Substrate Recognition and Active Site Dynamics. Biochemistry, 2014, 53, 7794-7804.	1.2	8
70	Kinetic and Structural Characterization of Tunnel-Perturbing Mutants in <i>Bradyrhizobium japonicum</i> Proline Utilization A. Biochemistry, 2014, 53, 5150-5161.	1.2	19
71	Structure, mechanism, and dynamics of UDP-galactopyranose mutase. Archives of Biochemistry and Biophysics, 2014, 544, 128-141.	1.4	49
72	Evidence That the C-Terminal Domain of a Type B PutA Protein Contributes to Aldehyde Dehydrogenase Activity and Substrate Channeling. Biochemistry, 2014, 53, 5661-5673.	1.2	18

#	Article	IF	CITATIONS
73	Structural Studies of Yeast Δ ¹ -Pyrroline-5-carboxylate Dehydrogenase (ALDH4A1): Active Site Flexibility and Oligomeric State. Biochemistry, 2014, 53, 1350-1359.	1.2	30
74	Substrateâ€dependent dynamics of UDPâ€galactopyranose mutase: Implications for drug design. Protein Science, 2013, 22, 1490-1501.	3.1	11
75	Solution structures of polcalcin Phl p 7 in three ligation states: Apoâ€, hemiâ€Mg ²⁺ â€bound, and fully Ca ²⁺ â€bound. Proteins: Structure, Function and Bioinformatics, 2013, 81, 300-315.	1.5	12
76	Structural Determinants of Oligomerization of Δ1-Pyrroline-5-Carboxylate Dehydrogenase: Identification of a Hexamerization Hot Spot. Journal of Molecular Biology, 2013, 425, 3106-3120.	2.0	24
77	Structural basis of substrate selectivity of Δ1-pyrroline-5-carboxylate dehydrogenase (ALDH4A1): Semialdehyde chain length. Archives of Biochemistry and Biophysics, 2013, 538, 34-40.	1.4	24
78	Involvement of the β3-α3 Loop of the Proline Dehydrogenase Domain in Allosteric Regulation of Membrane Association of Proline Utilization A. Biochemistry, 2013, 52, 4482-4491.	1.2	17
79	Targeting UDP-Galactopyranose Mutases from Eukaryotic Human Pathogens. Current Pharmaceutical Design, 2013, 19, 2561-2573.	0.9	19
80	2 PutA and proline metabolism. , 2012, , 31-56.		1
81	Crystal Structures and Small-angle X-ray Scattering Analysis of UDP-galactopyranose Mutase from the Pathogenic Fungus Aspergillus fumigatus. Journal of Biological Chemistry, 2012, 287, 9041-9051.	1.6	33
82	Identification of the NAD(P)H Binding Site of Eukaryotic UDP-Galactopyranose Mutase. Journal of the American Chemical Society, 2012, 134, 18132-18138.	6.6	25
83	Crystal Structures and Kinetics of Monofunctional Proline Dehydrogenase Provide Insight into Substrate Recognition and Conformational Changes Associated with Flavin Reduction and Product Release. Biochemistry, 2012, 51, 10099-10108.	1.2	31
84	Crystal Structures ofTrypanosoma cruziUDP-Galactopyranose Mutase Implicate Flexibility of the Histidine Loop in Enzyme Activation. Biochemistry, 2012, 51, 4968-4979.	1.2	23
85	The Three-Dimensional Structural Basis of Type II Hyperprolinemia. Journal of Molecular Biology, 2012, 420, 176-189.	2.0	57
86	Conservation of Functionally Important Global Motions in an Enzyme Superfamily across Varying Quaternary Structures. Journal of Molecular Biology, 2012, 423, 831-846.	2.0	13
87	Unique structural features and sequence motifs of proline utilization A (PutA). Frontiers in Bioscience - Landmark, 2012, 17, 556.	3.0	27
88	Proline: Mother Nature's cryoprotectant applied to protein crystallography. Acta Crystallographica Section D: Biological Crystallography, 2012, 68, 1010-1018.	2.5	28
89	The Biological Buffer Bicarbonate/CO ₂ Potentiates H ₂ O ₂ -Mediated Inactivation of Protein Tyrosine Phosphatases. Journal of the American Chemical Society, 2011, 133, 15803-15805.	6.6	57
90	Crystal structure and immunogenicity of the class C acid phosphatase from Pasteurella multocida. Archives of Biochemistry and Biophysics, 2011, 509, 76-81.	1.4	4

#	Article	IF	CITATIONS
91	Steady-state kinetic mechanism of the proline:ubiquinone oxidoreductase activity of proline utilization A (PutA) from Escherichia coli. Archives of Biochemistry and Biophysics, 2011, 516, 113-120.	1.4	43
92	Quaternary structure, conformational variability and global motions of phosphoglucosamine mutase. FEBS Journal, 2011, 278, 3298-3307.	2.2	10
93	Structural basis of the inhibition of class C acid phosphatases by adenosine 5′â€phosphorothioate. FEBS Journal, 2011, 278, 4374-4381.	2.2	2
94	Redox Regulation of Protein Tyrosine Phosphatases: Structural and Chemical Aspects. Antioxidants and Redox Signaling, 2011, 15, 77-97.	2.5	149
95	Expression, purification and crystallization of an atypical class C acid phosphatase fromMycoplasma bovis. Acta Crystallographica Section F: Structural Biology Communications, 2011, 67, 1296-1299.	0.7	2
96	Solution structures of chicken parvalbumin 3 in the Ca ²⁺ â€free and Ca ²⁺ â€bound states. Proteins: Structure, Function and Bioinformatics, 2011, 79, 752-764.	1.5	7
97	Crystal structure of a bacterial phosphoglucomutase, an enzyme involved in the virulence of multiple human pathogens. Proteins: Structure, Function and Bioinformatics, 2011, 79, 1215-1229.	1.5	29
98	Small-angle X-ray Scattering Studies of the Oligomeric State and Quaternary Structure of the Trifunctional Proline Utilization A (PutA) Flavoprotein from Escherichia coli. Journal of Biological Chemistry, 2011, 286, 43144-43153.	1.6	17
99	Crystal structure of the bifunctional proline utilization A flavoenzyme from <i>Bradyrhizobium japonicum</i> . Proceedings of the National Academy of Sciences of the United States of America, 2010, 107, 2878-2883.	3.3	59
100	The Structure of the Proline Utilization A Proline Dehydrogenase Domain Inactivated by N-Propargylglycine Provides Insight into Conformational Changes Induced by Substrate Binding and Flavin Reduction,. Biochemistry, 2010, 49, 560-569.	1.2	36
101	Structure of Avian Thymic Hormone, a High-Affinity Avian β-Parvalbumin, in the Ca2+-Free and Ca2+-Bound States. Journal of Molecular Biology, 2010, 397, 991-1002.	2.0	8
102	Recognition of Nucleoside Monophosphate Substrates by Haemophilus influenzae Class C Acid Phosphatase. Journal of Molecular Biology, 2010, 404, 639-649.	2.0	14
103	Characterization of a Unique Class C Acid Phosphatase from <i>Clostridium perfringens</i> . Applied and Environmental Microbiology, 2009, 75, 3745-3754.	1.4	17
104	Expression, purification and crystallization of class C acid phosphatases fromFrancisella tularensisandPasteurella multocida. Acta Crystallographica Section F: Structural Biology Communications, 2009, 65, 226-231.	0.7	3
105	A structurally conserved water molecule in Rossmann dinucleotide-binding domains. Protein Science, 2009, 11, 2125-2137.	3.1	138
106	A Conserved Active Site Tyrosine Residue of Proline Dehydrogenase Helps Enforce the Preference for Proline over Hydroxyproline as the Substrate. Biochemistry, 2009, 48, 951-959.	1.2	30
107	Functional Role for the Conformationally Mobile Phenylalanine 223 in the Reaction of Methylenetetrahydrofolate Reductase from <i>Escherichia coli</i> . Biochemistry, 2009, 48, 7673-7685.	1.2	19
108	Crystal Structures of the Histidine Acid Phosphatase from Francisella tularensis Provide Insight into Substrate Recognition. Journal of Molecular Biology, 2009, 394, 893-904.	2.0	12

#	Article	IF	CITATIONS
109	Energetics of OCP1–OCP2 complex formation. Biophysical Chemistry, 2008, 134, 64-71.	1.5	18
110	Structural biology of proline catabolism. Amino Acids, 2008, 35, 719-730.	1.2	136
111	Three crystal forms of the bifunctional enzyme proline utilization A (PutA) fromBradyrhizobium japonicum. Acta Crystallographica Section F: Structural Biology Communications, 2008, 64, 949-953.	0.7	8
112	Solution structure of Ca ²⁺ â€free rat αâ€parvalbumin. Protein Science, 2008, 17, 431-438.	3.1	25
113	Structural Basis of the Transcriptional Regulation of the Proline Utilization Regulon by Multifunctional PutA. Journal of Molecular Biology, 2008, 381, 174-188.	2.0	62
114	Structural Basis for the Inactivation of Thermus thermophilus Proline Dehydrogenase by <i>N-</i> Propargylglycine [,] . Biochemistry, 2008, 47, 5573-5580.	1.2	25
115	Structure and Kinetics of Monofunctional Proline Dehydrogenase from Thermus thermophilus. Journal of Biological Chemistry, 2007, 282, 14316-14327.	1.6	88
116	Crystallization of Phi29 Spindle-Shaped Nano-Bar Anti-Receptor with Glycosidase Domain. Journal of Nanoscience and Nanotechnology, 2007, 7, 2616-2622.	0.9	2
117	Impact of DNA Hairpin Folding Energetics on Antibody–ssDNA Association. Journal of Molecular Biology, 2007, 374, 1029-1040.	2.0	14
118	Redox-Induced Changes in Flavin Structure and Roles of Flavin N(5) and the Ribityl 2â€~-OH Group in Regulating PutAâ^'Membrane Bindingâ€,‡. Biochemistry, 2007, 46, 483-491.	1.2	51
119	Structure of Recombinant Haemophilus Influenzae e (P4) Acid Phosphatase Reveals a New Member of the Haloacid Dehalogenase Superfamily,. Biochemistry, 2007, 46, 11110-11119.	1.2	14
120	Solution structure of Ca ²⁺ â€free rat βâ€parvalbumin (oncomodulin). Protein Science, 2007, 16, 1914-1926.	3.1	33
121	Desulfovibrio desulfuricans G20 Tetraheme Cytochrome Structure at 1.5Ã and Cytochrome Interaction with Metal Complexes. Journal of Molecular Biology, 2006, 358, 1314-1327.	2.0	15
122	Characterization of recombinant Francisella tularensis acid phosphatase A. Protein Expression and Purification, 2006, 45, 132-141.	0.6	27
123	High-resolution structure of humanD-glyceraldehyde-3-phosphate dehydrogenase. Acta Crystallographica Section D: Biological Crystallography, 2006, 62, 290-301.	2.5	108
124	Crystallization of a newly discovered histidine acid phosphatase fromFrancisella tularensis. Acta Crystallographica Section F: Structural Biology Communications, 2006, 62, 32-35.	0.7	7
125	Crystallization of recombinantHaemophilus influenzaee(P4) acid phosphatase. Acta Crystallographica Section F: Structural Biology Communications, 2006, 62, 464-466.	0.7	7
126	Cloning, purification and crystallization ofBacillus anthracisclass C acid phosphatase. Acta Crystallographica Section F: Structural Biology Communications, 2006, 62, 705-708.	0.7	19

#	Article	IF	CITATIONS
127	Exploring structurally conserved solvent sites in protein families. Proteins: Structure, Function and Bioinformatics, 2006, 64, 404-421.	1.5	34
128	Crystal structures of the DNA-binding domain ofEscherichia coliproline utilization A flavoprotein and analysis of the role of Lys9 in DNA recognition. Protein Science, 2006, 15, 2630-2641.	3.1	38
129	Structure of Francisella tularensis AcpA. Journal of Biological Chemistry, 2006, 281, 30289-30298.	1.6	67
130	Crystallization of AcpA, a respiratory burst-inhibiting acid phosphatase from Francisella tularensis. Biochimica Et Biophysica Acta - Proteins and Proteomics, 2005, 1752, 107-110.	1.1	11
131	Cloning, purification and crystallization ofThermus thermophilusproline dehydrogenase. Acta Crystallographica Section F: Structural Biology Communications, 2005, 61, 737-739.	0.7	6
132	Crystal Structure of the D94S/G98E Variant of Rat α-Parvalbumin. An Explanation for the Reduced Divalent Ion Affinityâ€. Biochemistry, 2005, 44, 10966-10976.	1.2	4
133	Evidence for Structural Plasticity of Heavy Chain Complementarity-determining Region 3 in Antibody–ssDNA Recognition. Journal of Molecular Biology, 2005, 347, 965-978.	2.0	28
134	Identification and Characterization of the DNA-binding Domain of the Multifunctional PutA Flavoenzyme. Journal of Biological Chemistry, 2004, 279, 31171-31176.	1.6	46
135	Structure of an anti-DNA fab complexed with a non-DNA ligand provides insights into cross-reactivity and molecular mimicry. Proteins: Structure, Function and Bioinformatics, 2004, 57, 269-278.	1.5	15
136	Detection ofL-lactate in polyethylene glycol solutions confirms the identity of the active-site ligand in a proline dehydrogenase structure. Acta Crystallographica Section D: Biological Crystallography, 2004, 60, 985-986.	2.5	4
137	Probing a hydrogen bond pair and the FAD redox properties in the proline dehydrogenase domain of Escherichia coli PutA. Biochimica Et Biophysica Acta - Proteins and Proteomics, 2004, 1701, 49-59.	1.1	14
138	Crystal Structure of a High-Affinity Variant of Rat α-Parvalbuminâ€. Biochemistry, 2004, 43, 10008-10017.	1.2	16
139	Structures of theEscherichia coliPutA Proline Dehydrogenase Domain in Complex with Competitive Inhibitorsâ€,‡. Biochemistry, 2004, 43, 12539-12548.	1.2	74
140	Crystal structure of rat α-parvalbumin at 1.05 à resolution. Protein Science, 2004, 13, 1724-1734.	3.1	28
141	MRSAD: using anomalous dispersion from S atoms collected at Cuâ€Kα wavelength in molecular-replacement structure determination. Acta Crystallographica Section D: Biological Crystallography, 2003, 59, 1731-1736.	2.5	30
142	Structure of the proline dehydrogenase domain of the multifunctional PutA flavoprotein. Nature Structural Biology, 2003, 10, 109-114.	9.7	96
143	Crystal structure of an antigen-binding fragment bound to single-stranded DNA 1 1Edited by I. A. Wilson. Journal of Molecular Biology, 2001, 314, 807-822.	2.0	56
144	Crystallization and preliminary crystallographic analysis of the proline dehydrogenase domain of the multifunctional PutA flavoprotein fromEscherichia coli. Acta Crystallographica Section D: Biological Crystallography, 2001, 57, 1925-1927.	2.5	13

#	Article	IF	CITATIONS
145	Conformations of nicotinamide adenine dinucleotide (NAD+) in various environments. , 2000, 13, 27-34.		27
146	Crystallization and molecular-replacement studies of a recombinant antigen-binding fragment complexed with single-stranded DNA. Acta Crystallographica Section D: Biological Crystallography, 2000, 56, 1007-1011.	2.5	5
147	Unusual folded conformation of nicotinamide adenine dinucleotide bound to flavin reductase P. Protein Science, 1999, 8, 1725-1732.	3.1	45
148	Molecular Dynamics Simulations of NAD+in Solution. Journal of the American Chemical Society, 1999, 121, 8637-8644.	6.6	29
149	Structure of Bacterial Luciferase β2 Homodimer:  Implications for Flavin Binding,. Biochemistry, 1997, 36, 665-672.	1.2	18
150	Determinants of Enzyme Thermostability Observed in the Molecular Structure of Thermus aquaticus d-Glyceraldehyde-3-phosphate Dehydrogenase at 2.5 Ã Resolution,. Biochemistry, 1996, 35, 2597-2609.	1.2	216
151	Flavin Reductase P:  Structure of a Dimeric Enzyme That Reduces Flavin,. Biochemistry, 1996, 35, 13531-13539.	1.2	98
152	Preliminary crystallographic analysis of glyceraldehyde 3-phosphate dehydrogenase from the extreme thermophile Thermus aquaticus. Acta Crystallographica Section D: Biological Crystallography, 1994, 50, 744-748.	2.5	4
153	Molecular dynamics simulations and rigid body (TLS) analysis of aspartate carbamoyltransferase: Evidence for an uncoupled R state. Protein Science, 1993, 2, 927-935.	3.1	20
154	A comparative study of time dependent quantum mechanical wave packet evolution methods. Journal of Chemical Physics, 1992, 96, 2077-2084.	1.2	73
155	Anti-insulin antibody structure and conformation. II. Molecular dynamics with explicit solvent. Biopolymers, 1992, 32, 23-32.	1.2	24
156	Ab initio study of proton transfer in [H3Nâ^'Hâ^'NH3]+ and [H3Nâ^'Hâ^'OH2]+. Chemical Physics Letters, 1990, 175, 282-288.	1.2	70
157	A computer-based approach to teaching quantum dynamics. Journal of Chemical Education, 1990, 67, 917.	1.1	23
158	Floquet analysis of the far-infrared dissociation of a Morse oscillator. Physical Review A, 1989, 40, 4054-4064.	1.0	23
159	Far IR dissociation of a highly excited Morse oscillator. Chemical Physics Letters, 1988, 149, 503-509.	1.2	9
160	The role of rotation in the vibrational relaxation of diatomic molecules. Chemical Physics, 1988, 119, 307-324.	0.9	10
161	A modified landau-teller model for vibrational relaxation of small molecular ions. Chemical Physics Letters, 1987, 138, 495-502.	1.2	23